Short communication

Direct three-dimensional reconstruction of a nanoporous catalyst layer for a polymer electrolyte fuel cell

Christoph Ziegler*, Simon Thiele, Roland Zengerle

Laboratory for MEMS Applications, Department of Microsystems Engineering (IMTEK), *University of Freiburg, Georges-Koehler-Allee 106, 79110 Freiburg, Germany*

ABSTRACT

The direct three-dimensional reconstruction of a polymer electrolyte fuel cell cathode catalyst layer from focused ion beam/scanning electron microscope (FIB/SEM) images is presented. The carbon and pore distribution is shown and quantitatively analysed. A new catalyst layer sample (Fumapem-F950/HiSpec13100) is sliced with FIB and a series of SEM images is taken. The images are registered, segmented and a three-dimensional stack is reconstructed. The three-dimensional carbon and pore distribution is shown. Based on the reconstruction the pore size distribution is evaluated. The total porosity and the unconnected pores space is analysed. The fully segmented 2D images are provided as supplemental material to this paper for future analysis and modeling work.

© 2010 Elsevier B.V. All rights reserved.

1. Introduction

The introduction of hybrid electric vehicles has prepared the complete replacement of gasoline systems by systems based on batteries or polymer-electrolyte fuel cells [1]. Progress has been made in the design of fuel cell materials and components such as bipolar plates and flow fields, gas diffusion layers, membranes and catalyst layers [2]. However, performance loss and degradation still occurs in the catalyst layer, which is impeding its application. While one research direction aims to solve the major challenges by exploring new materials [3], there is also a great need for detailed insight into materials to exploit the potential for significant increase in performance and durability. The introduction of new analytical methods for morphology is very important in this context since the coupled transport of oxygen, water, protons and electrons is decisive for the electrochemical conversion performance of the catalyst layer. The characteristic pore sizes range from a few nm to almost 1 μm. The spatial resolution of X-ray tomography is too low for investigating the catalyst layer in detail whereas transmission electron microscopy is suited for investigations of catalyst features in the range of a few nm and does not allow for visualization of larger areas [4]. The focused ion beam/scanning electron microscope (FIB/SEM) tomography recently emerged [5] and has been used for a variety of materials including ceramic fuel cells [6–8]. Up to now however there has not been a three-dimensional reconstruction of a polymer electrolyte fuel cell catalyst layer. For the first time, we present here the three-dimensional morphology of

a catalyst layer for a polymer-electrolyte fuel cell, which is based directly on highly sensitive FIB/SEM analysis.

2. Catalyst layer morphology and species transport

Imaging methods such as X-ray and neutron tomography provide detailed insight into the distribution of water in flow channels and gas diffusion layers. The catalyst layer where the electrochemical conversion takes place is by far the most complex layer. It contains two conductive phases for electrons and protons and has a pore size distribution ranging from the nano-scale to the micro-scale for two-phase transport. An attempt has been made to model the complex behaviour of the catalyst layer and its relation to fuel cell performance [9,10]. However, compared to the gas diffusion layer, knowledge about transport properties of the catalyst layer is limited. A major gap is the lack of an experimental method for direct observation of two-phase transport in pores below the micro-scale. This has led to a situation where knowledge about the transport properties of fuel cell components is driven by accessibility rather than importance. Unlike the gas diffusion layer, the transport properties of the catalyst layer cannot be measured in a straightforward manner, because the catalyst layer is an ultra-thin layer coated onto the membrane. Thus, important material properties can be obtained only from a realistic model of the catalyst layer.

Modelling plays an important role in designing and understanding fuel cells and has led to major improvements. The design of flow fields, individual cells and fuel cell stacks is enhanced by computational fluid dynamics [11]. Major progress has been made in understanding the role of the gas diffusion layer, consisting of a micro-porous material for the distribution of reactants, electrical contact and mechanical support. The gas diffusion layer is well-
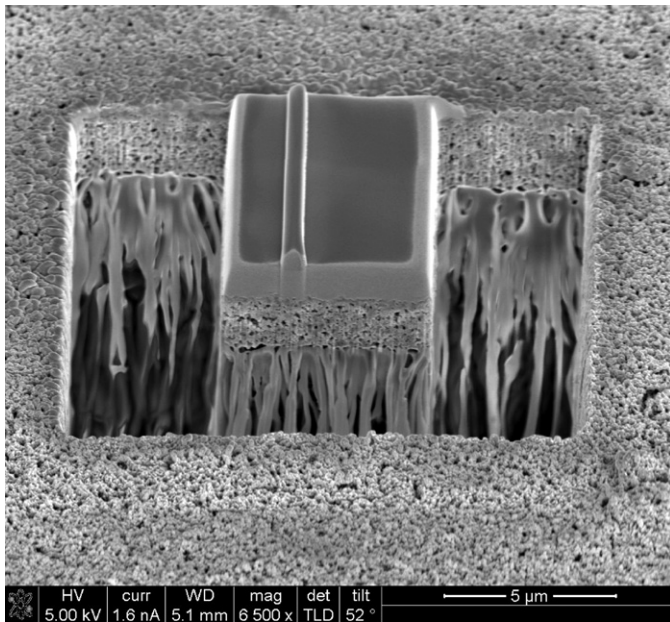

Fig. 1. Preparation of the catalyst layer sample. The region of interest under the protecting strip is cut clear from the pristine sample. The cut through the catalyst layer is clean whereas the underlying polymer membrane is damaged by the high energy density of the ion beam used for the preparation. For the fine slicing the energy density of the beam is reduced.

defined in terms of the relation between its structure and transport properties such as the permeability [12]. The behaviour of micro-porous and nano-porous media can be described in terms of porous medium theory that treats the materials as homogeneous with respect to the reference elementary volume under consideration [13,14]. This is a valuable approach for the understanding of multi-layer assemblies and the dynamic behaviour that generally cannot be described by particle-based simulation methods such as molecular dynamics [15,16]. The description of two-phase transport relies on the use of homogenized material properties such as poros-

ity, diffusivity and permeability. Some of these properties depend strongly on the degree of liquid saturation in the network of pores. The two-phase transport equation for a porous medium is

$$\partial_t \left[\pi_\kappa \rho_j s_j \right] + \nabla \cdot \left[\rho_j v \right] = Q_j \tag{1}$$

$$v_j = -K_\kappa \frac{k_j}{\mu_j} \nabla p_j \tag{2}$$

where ρ denotes the phase density of phase j, s the saturation and v the phase velocity, respectively. Q is a phase-specific mass source term that can be used to describe phase transitions and electro-chemical reactions. The phase velocity depends on the viscosity μ and the phase pressure gradient p. The material properties that are decisive for the efficiency of the two-phase flow are the porosity π of the material κ, the absolute permeability K and the relative permeability k. The relative permeability depends strongly on the saturation of the medium.

Measurements to determine these parameters have their limitations. The determination of surface areas with the Brunauer–Emmett–Teller method requires a larger surface area and often porosity data is unreliable for nanoporous media of mixed wettability. The pore size distribution, a fundamental material property, is unavailable for catalyst layers. Moreover, there is no clear concept of the underlying physics in the catalyst layer. The fraction of pores for which the continuum assumption holds is unknown and thus the application of appropriate models for the respective regions in the catalyst layer is difficult. Thus, this paper aims to prepare the ground for the next generation of models and novel structures for the catalyst layer of polymer-electrolyte fuel cells by providing a direct three-dimensional reconstruction of its morphology.

3. Materials and methods

A FuMa-Tech fumapem F-950 membrane (EW 950), which is a per-fluorinated sulphonic acid (PFSA)-PTFE copolymer, was investigated. The electrodes were produced by printing the membrane with a slurry containing 70 wt% platinum on HiSPEC 13100, a high surface-area carbon support obtained from Johnson Matthey using
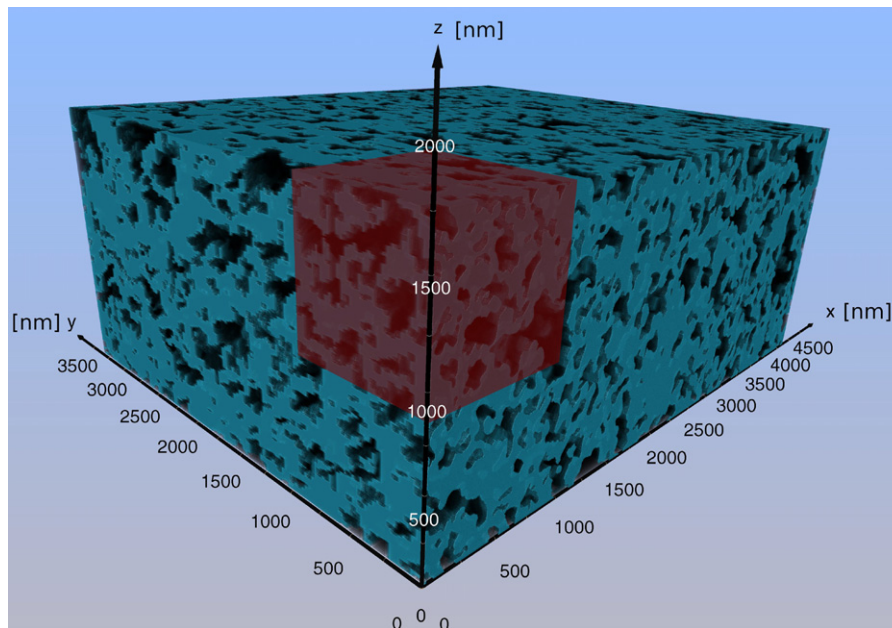

Fig. 2. Three-dimensional reconstruction of a polymer-electrolyte fuel cell catalyst layer. The reconstruction is based on 113 SEM images obtained with a separation of 30 nm. The layer is a highly porous carbon network with well-connected pores that form continuous pathways within the layer. The side-length of the geometry is 4.13 µl in the x direction, 1.75 µm in the z-direction and 3.39 µm in the y-direction.
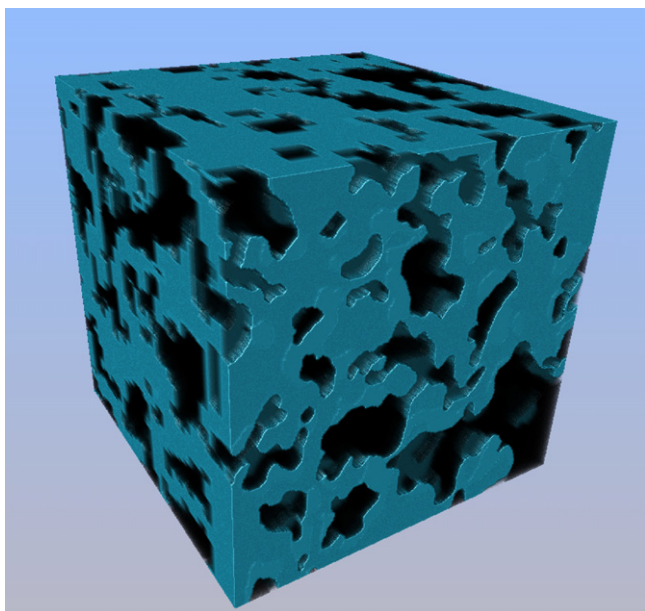
Fig. 3. Detail of the solid phase volume fraction. The illustrated volume is indicated in red in Fig. 2. The side length of the cube is 900 nm. (For interpretation of the references to color in this figure legend, the reader is referred to the web version of the article.)

an EKRA screen printer. Multiple prints were applied to ensure appropriate catalyst loading. A 20% Nafion dispersion from DuPont was used as an ionomer and was mixed into the paste in an Ultra Turrax (IKA T25 digital) to obtain approximately 20% solid material in the paste. The screen printing process resulted in a catalyst layer thickness of ca. 2 μm (Fig. 1). After air drying, the catalyst layer was cured at 130 °C in a drying oven. The catalyst layer was used in pristine state with no features that are caused by a specific operation protocol. The sample was investigated with a dual-beam FIB/SEM instrument (FEI Quanta 3D), following a procedure similar to that described for ceramic and chalk materials [17,18]. After initial preparation, the exposed surface (Fig. 1) was removed in 113 slices with a very sensitive feed of 30 nm. This was
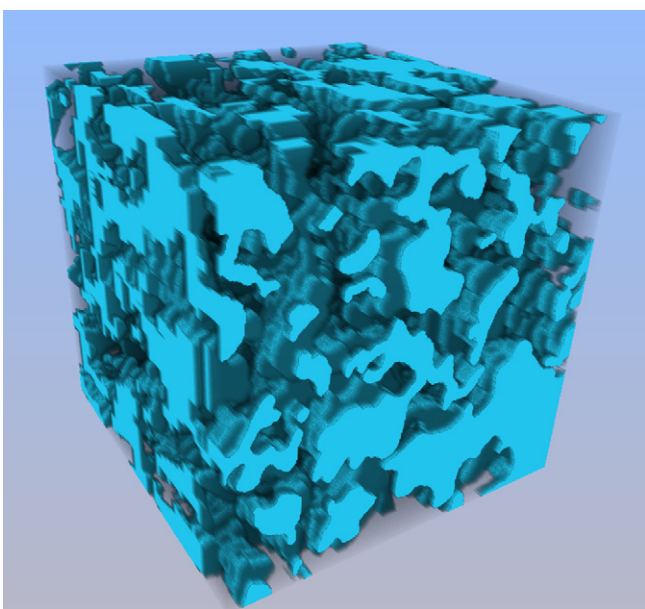

Fig. 4. Complementary pore space. The pore space is highlighted here in a complementary image to Fig. 3. This image shows the good connectivity of the pores and some minor isolated pores.
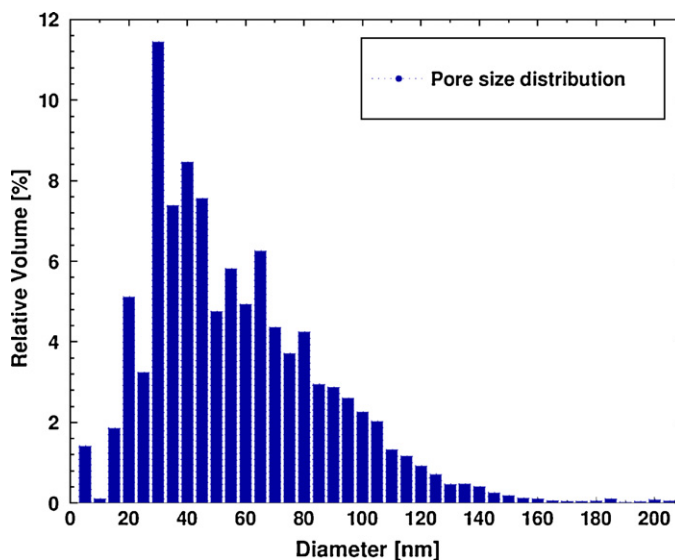

Fig. 5. Pore size distribution. Histogram of the percentage of pore space volume versus the local pore diameters determined from the reconstructed image of Fig. 2.

followed by SEM imaging under high vacuum of the surface for each slice. Each individual SEM image was registered with ImageJ (http://rsb.info.nih.gov/ij/) in combination with the "StackReg" plug-in [19] (http://bigwww.epfl.ch/thevenaz/stackreg/). During pre-processing in Matlab (2009a), the images were vertically stretched by a factor of 1.27 to compensate for the angle of 52° between SEM and FIB. Segmentation was done with the "gimp" open-source code (http://www.gimp.org/).

4. Results

The three-dimensional reconstruction of the catalyst layer is shown in Fig. 2. The reconstruction reveals the highly porous structure of the carbon matrix. There is a well-connected network of pores for reactant transport that offers a variety of continuous pathways through the layer. The pore size shows significant local variation. A cut-out is defined to display the detailed morphology of the two phases. In Fig. 3, the nano-porosity of the carbon is clearly visible. For comparison, Fig. 4 shows the complementary pore space, which forms a connected pore network but also indicates that there are some isolated pores. Platinum located in unconnected pore space is lost to the electrochemical reaction and hence has a direct impact on the performance of the material. For this sample, the fraction of unconnected pores is determined to be only 0.56% of the total pore volume and is thus negligible. Based in Fig. 3, the total porosity is determined to be 38%, with the volume fraction of carbon thus being 62%. To further evaluate the characteristics of the material, the pore size distribution according to Delerue et al. [20] was determined (Fig. 5), which shows the relative frequency of the pore space volume as a function of the pore diameter.

5. Conclusion

For the first time, an approach to visualise the three-dimensional morphology of a polymer-electrolyte fuel cell catalyst layer has been demonstrated. The feasibility of a FIB/SEM analysis has been shown on a FuMa-Tech fumapem F-950 membrane (EW 950) coated with HiSPEC 13100/Nafion. The results show the three-dimensional distribution of the carbon phase and the pore space. Based on the reconstruction the pore size distribution was determined. The segmented two-dimensional images are provided as supplementary material for further analysis such as determination of the relative gas permeability.

Future applications include the investigation of morphology change due to carbon corrosion and the change of pore size distribution due to shelf life and operation. A comparative study of different materials will greatly increase knowledge of ageing and related morphological changes. The geometrical configuration obtained is the basis for simulating transport mechanisms with unprecedented accuracy and determining parametrizations for use in numerical up-scaling. Moreover, this work makes a contribution to the overall concept of virtual material design, which combines three-dimensional reconstruction, transport simulation and performance prediction on the one hand with materials processing and electrochemical characterization on the other.

Acknowledgements

Appendix A. Supplementary data

Supplementary data associated with this article can be found, in the online version, at doi:10.1016/j.jpowsour.2010.09.044.

References

[1] S. Dunn, Int. J. Hydrogen Energy 27 (2002) 235–264.
[2] B.C.H. Steele, A. Heinzel, Nature 414 (2001) 345–352.
[3] G.G. Wallace, J. Chen, A.J. Mozer, M. Forsyth, D.R. MacFarlane, C.Y. Wang, Mater. Today 12 (2009) 20–27.
[4] G. Möbus, B. Inkson, Mater. Today 10 (12) (2007) 18–25.
[5] L. Holzer, F. Indutnyi, P. Gasser, B. Munch, M. Wegmann, J. Microsc. 216 (1) (2004) 84.
[6] S. Cao, W. Tirry, W. Van den Broek, D. Schryvers, J. Microsc. 233 (1) (2009) 61–68.
[7] J. Wilson, W. Kobsiriphat, R. Mendoza, H. Chen, J. Hiller, D. Miller, K. Thornton, P. Voorhees, S. Adler, S. Barnett, Nat. Mater. 5 (7) (2006) 541–544.
[8] D. Gostovic, J. Smith, D. Kundinger, K. Jones, E. Wachsman, Electrochem. Solid-State Lett. 10 (2007) B214.
[9] D. Gerteisen, T. Heilmann, C. Ziegler, J. Power Sources 187 (2009) 165–181.
[10] J. Liu, M. Eikerling, Electrochim. Acta 53 (2008) 4435–4446.
[11] S. Shimpalee, M. Ohashi, J.W. Van Zee, C. Ziegler, C. Sadeler, C. Stoeckmann, C. Hebling, Electrochim. Acta 54 (2009) 2899–2911.
[12] P.K. Sinha, P.P. Mukherjee, C.Y. Wang, J. Mater. Chem. 17 (2007) 3089–3103.
[13] Z.H. Wang, C.Y. Wang, K.S. Chen, J. Power Sources 94 (2001) 40–50.
[14] C. Ziegler, D. Gerteisen, J. Power Sources 188 (2009) 184–191.
[15] M. Gad-el-Hak, Phys. Fluids 17 (2005) 100612.
[16] M. Gad-el-Hak, Heat Trans. Eng. 27 (2006) 13–29.
[17] J.R. Wilson, W. Kobsiriphat, R. Mendoza, Nat. Mater. 5 (2006) 541–544.
[18] L. Tomutsa, D. Silin, V. Radmilovic, SPE Reservoir Eval. Eng. 10 (2007) 285–293.
[19] P. Thévenaz, U.E. Ruttimann, M. Unser, IEEE Trans. Image Process. 7 (1998) 27–41.
[20] J.F. Delerue, E. Perrier, Z.Y. Yu, B. Velde, Phys. Chem. Earth Part A 24 (1999) 639–644.